Orthodontics & Craniofacial Research

ORIGINAL ARTICLE

Visual pathway-related horizontal reference plane for three-dimensional craniofacial analysis

*Y. H. Kang**
*B. C. Kim**
K. R. Park
J. Y. Yon
H. J. Kim
H. J. Tak
Z. Piao
M. K. Kim
S. H. Lee

Authors' affiliations:
Y. H. Kang, K. R. Park, H. J. Kim, S. H. Lee, Department of Oral and Maxillofacial Surgery, College of Dentistry, Yonsei University, Seoul, Korea
B. C. Kim, Department of Oral and Maxillofacial Surgery, Daejeon Dental Hospital, College of Dentistry, Wonkwang University, Daejeon, Korea
J. Y. Yon, Department of Periodontology, Research Institute for Periodontal Regeneration, College of Dentistry, Yonsei University, Seoul, Korea
H. J. Tak, Department of Applied Life Science, Brain Korea 21 Project, College of Dentistry, Yonsei University, Seoul, Korea
Z. Piao, Department of Oral and Maxillofacial Surgery, Stomatology Hospital of Guangzhou Medical College, GuangZhou City, Guang Dong Province, China
M. K. Kim, Department of Oral and Maxillofacial Surgery, National Health Insurance Corporation Ilsan Hospital, Goyang, Korea

Correspondence to:
Sang-Hwy Lee
Department of Oral and Maxillofacial Surgery and Applied Life Science
Oral Science Research Cente, College of Dentistry Yonsei University,
50 Yonsei-ro
Seodaemun-Gu, Seoul 120-752, Korea
E-mail: sanghwy@yuhs.ac

*YH Kang and BC Kim contributed equally to this study.

Date:
Accepted 9 June 2012

DOI: 10.1111/j.1601-6343.2012.01551.x

Kang Y. H., Kim B. C., Park K. R., Yon J. Y., Kim H. J., Tak H. J., Piao Z., Kim M. K., Lee S. H. Visual pathway-related horizontal reference plane for three-dimensional craniofacial analysis
Orthod Craniofac Res 2012;**15**:245–254. © 2012 John Wiley & Sons A/S

Structured Abstract

Authors – Kang YH, Kim BC, Park KR, Yon JY, Kim HJ, Tak HJ, Piao Z, Kim MK, Lee SH

Objectives – To construct three-dimensional (3D) horizontal reference planes based on visual pathway and to determine their stability and reliability by analyzing the structural patterns of normal and dysmorphology for 3D craniofacial analysis.

Setting and Sample Population – Thirty-six subjects with maxillofacial dysmorphology and malocclusion, and eight normal controls.

Materials and Methods Population – On the 3D computed tomographic images of the subjects, the visual pathway-based planes, including the orbital axis plane (OAP), visual axis plane (VAP), and the optical axis plane (OpAP), were constructed and evaluated.

Results – The OAP, but not the VAP and OpAP, showed the ideal relationship between the midsagittal and posterior maxillary plane, and properly described the different patterns of maxillofacial dysmorphology with craniofacial plane 1 of Delaire's analysis and the occlusal plane.

Conclusions – The proposed visual pathway-related horizontal reference planes, and in particular the OAP, seem to correctly express the visual axis and the position of the head in natural head position and can be used as a horizontal reference plane for the 3D analysis of craniofacial dysmorphology and anthropology.

Key words: imaging; three-dimensional; natural head position; reference plane; tomography; X-ray computed; visual pathway

Introduction

Orthodontics, craniofacial surgery, and anthropometry focus on the detailed structural characteristics of maxillofacial deformities using various methods including the analyses of Delaire et al., Burstone et al., and Sassouni (1–3). Recent advances in three-dimensional (3D) visualization technology that combine computer graphics and digital imaging have improved analysis and treatment planning (4–6). Furthermore, the transformation of two-dimensional (2D) cephalometric analyses into 3D analyses has been validated showing that the difficulties were mainly related to the transposition of the reference points used in the analysis (7).

Achieving an accurate analysis of craniofacial structures with 3D computed tomography (CT) images basically requires reference planes as a baseline for the orientation of the head as well as the measurements, as for 2D analysis (8, 9). Furthermore, the 3D reference planes can be more critical because the baseline references provided by 3D CT are not as clear as those provided by 2D imaging, which are made with the help of head posture or orientation of the subjects (10). In addition, a 3D coordinate system of head position on 3D CT images inevitably differs on all occasions.

The Frankfort horizontal (FH) plane (11) or sella(S)-nasion(N) (12), which have been used most frequently for 2D analysis, are currently used as well for 3D analysis. Although the FH plane in 2D radiography has been used to express the natural head position (NHP), there is some disagreement regarding the descriptive ability for NHP (13, 14) as a result of the anatomical variability (15). Thus, it remains to be determined which planes are suitable and accurate for 3D craniofacial analysis (5, 6).

The NHP refers to the position of the head when a person maintains the balance of the head and looks at the horizon in a natural condition (16–18). Although NHP has been accepted as being the best horizontal reference plane in the fields of anthropology, art, and maxillofacial dysmorphology, its application has been limited because of difficulties in the configuration of the plane, especially in 2D radiography. Various methods have been suggested for the designation of the NHP (16, 19) and the introduction of 3D radiography has extended the capacity to set the NHP by the remarkably enhanced visibility of the anatomical structures, including optic foramen and orbital fissure (Fig. 1A).

Vision, or line of sight, is of great importance for the NHP. The upright stance and walking posture of a human, being a biped, makes the visual axis (VA) different from that of quadruped mammals (20). The VA is by definition a line that connects the lens of the eyeball and the retina's optic fovea (21), or the line between the lens and the retina when a person gazes to the horizon (Fig. 1B). The orbital axis (OA) refers to the line between the center of the orbit and the optic foramen of the optic canal (14) (Fig. 1C). The VA (as the yellow line in Fig. 1C) can be drawn to be nearly parallel to each other and the OA (as red dashed lines in Fig. 1C) bisects the medial and lateral orbital walls to make a converging angle of 45° (22).

According to Barbera et al., (16) the neutral horizontal axis refers to OA that fits the VA. Sassouni (3) introduced the concept of an OA for the NHP in his analysis. In addition, the neuro-ocular plane (NOP) is a cephalic reference plane expressing the visual pathway and defined as the one passing through lens, head of optic nerve, and optic canal (23). The horizontal nature of visual pathway and NOP was well demonstrated by Cabanis et al. (24) and Tamraz (23). Thus, it may be possible to construct the ideal horizontal reference plane by setting the VA- or OA-related plane (as VAP and OAP, respectively) for cephalic orientation and 3D morphometric analysis.

So we wanted to determine the visual pathway-related planes for the horizontal reference plane on 3D CT images. They were constructed and compared with some previously reported reference planes such as FH plane and the posterior maxillary (PM) plane of Enlow and Moyers (25).

Materials and methods

Subjects

The subjects were 36 individuals who visited the Department of Oral and Maxillofacial Surgery at

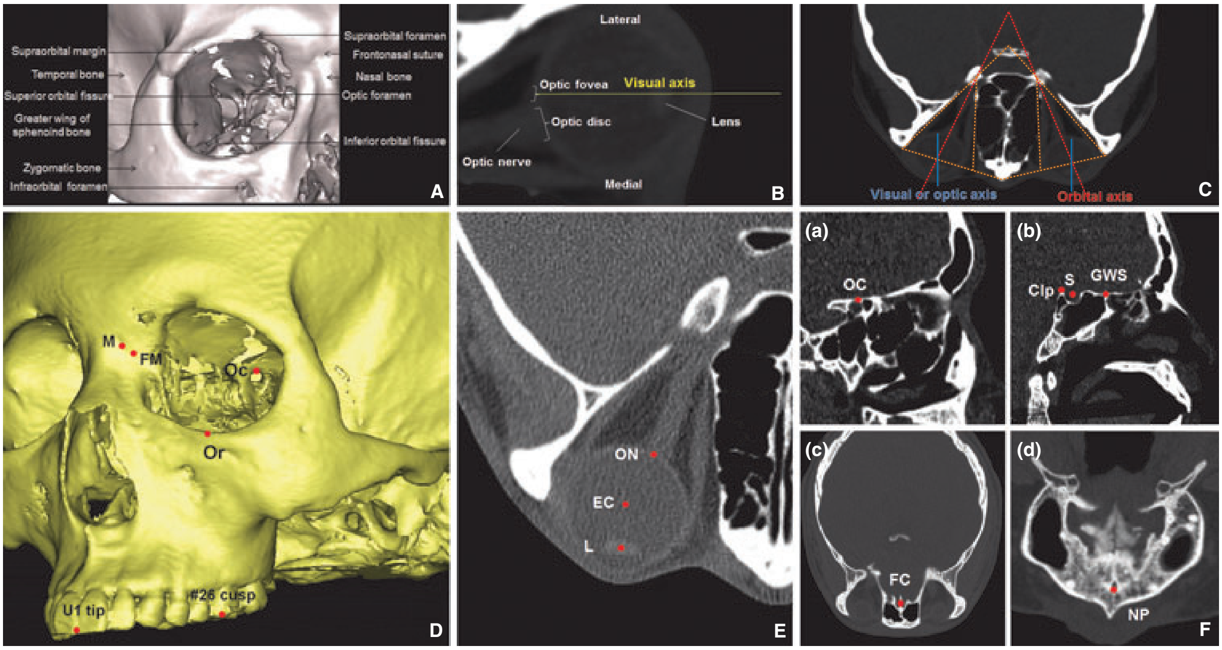

Fig. 1. Three-dimensional (3D) CT images of the eye-related structures with some reference points used in this study. (A) Frontal view of the bony orbit on 3D CT image. (B) The eyeball and optic nerve on the axial image of CT to present the visual axis (in yellow). (C) Drawing of the visual pathway-related orbital axis (in red) and visual or optic axis (in yellow) on the axial CT image, with the anatomical orbit and eyeball. (D–F) Some reference points used in this study. (D) The reference points at and around the orbit and maxilla of 3D CT image; FM (frontomaxillary suture), M (M point), OC (optic canal), Or (orbitale), PMF (pterygomaxillary fissure), U1 (tip of maxillary incisor), #26 (mesiobuccal cusp of left maxillary first molar). (E) Horizontal sectional image of the eyeball and orbit; ON (optic nerve), EC (eyeball center), L (lens). (F) Some reference points on the sagittal and axial images; (a) OC (optic canal), (b) Clp (posterior clinoid process), S (sella turica), GWS (greater wing of sphenoid), (c) FC (foramen cecum), (d) NP (nasopalatine canal).

the Dental Hospital of Yonsei University Health System, Seoul, Korea. Of these, 16 individuals had mandibular retrognathism (group II; mean age 22.5 years), and 20 subjects had mandibular prognathism (group III; mean age 19.7 years). The normal control (group I; mean age 20.2 years) comprised eight volunteers who had normal maxillofacial skeletal and occlusal patterns, as evidenced by clinical, occlusal, and cephalometric examinations. This work was approved by the local ethics committee of the Dental Hospital, Yonsei University Health System, Seoul, Korea (IRB number: 2-2009-0026).

Methods

Acquisition and reconstruction of 3D CT images

Each subject, with his FH line perpendicular to the floor, underwent CT imaging with a high-speed advantage CT system (GE Medical System, Milwaukee, WI, USA) using high-resolution bone algorithm protocol (200 mA, 120 kV, scanning time 1 s, 1-mm scan thickness, a 512×512-pixel reconstruction matrix, and a $0.48 \times 0.48 \times 1.0$-mm voxels). The CT image data, which were saved in the DICOM file format, were transferred to a personal computer and reconstructed into 3D skull images using Simplant Pro Crystal (Materialize Dental, Leuven, Belgium; Fig. 2). The subjects also underwent conventional 2D cephalometric radiography after adjustment of the head position to make it as close to the NHP as possible.

Setting the reference points and construction of the vision-based or other reference planes

One of authors set the reference points for subjects, achieving a total of 29 reference points (Table 1 and Fig. 1D–F). The lens, EC, and OC were used for the vision-based horizontal reference planes (Fig. 1D,E). As it was not possible to set the fovea on the 3D CT images (26), it was replaced with the ON, which is no different from the optic fovea in terms of its vertical location (Fig. 1B) (27). The following vision-based reference lines were constructed in this study: the OA, VA, and optical axis (OpA) lines (Fig. 1B,C).

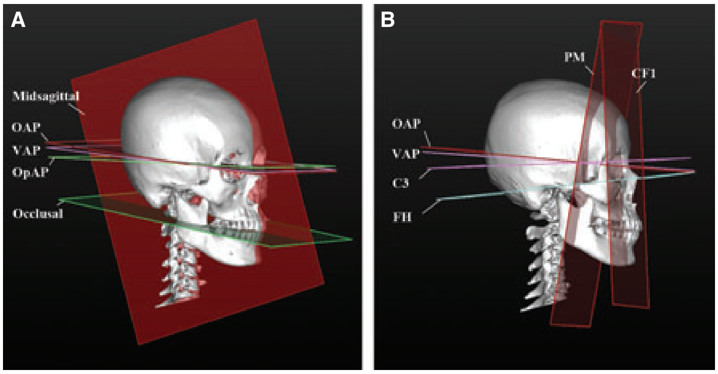

Fig. 2. The visual pathway-related planes and their relationship with other reference planes on the 3D CT images for a subject in group I. (A) Three visual pathway-related planes are shown with, from the top, OAP (orbital axis plane), VAP (visual axis plane), and OpAP (optical axis plane), together with the midsagittal and occlusal plane. (B) OAP and VAP are presented to be compared with other reference planes, including C3, FH, CF1, and the posterior maxillary (PM) planes.

The visual pathway-based plane was embodied by three planes including OAP, VAP, and optical axis plane (OpAP). They were constructed as described in Table 2, Figs 1C and 2, and the following reference planes were also constructed: MS, C3, CF1, FH, PM, and the occlusal plane (Table 2 and Fig. 2). The MS plane was set using the points of the foramen cecum, the center of the foramen magnum, and the sella and was augmented by the falx cerebri or Bregma (28). And the cranial plane 3 (C3) and craniofacial plane 1 (CF1) of Delaire's architectural and structural analysis, and the occlusal plane were also constructed as described (1, 4, 29).

Angular measurements and the statistical analysis

The angles between the reference planes (MS, PM, and others) and the vision-based planes (OAP, VAP, and OpAP) or lines (OA, VA, and OpA) were measured in groups I, II, and III. The results were first evaluated statistically by two-way analysis of variance (ANOVA) to determine whether there were any interclass correlations (ICCs) between the skeletal patterns and the measurement. If there were no ICCs, one-way ANOVA with *post hoc* analysis by Scheffe's method was performed for each result. The statistical analysis was carried out using SPSS for Windows (v. 12.0; SPSS, Cary, NC, USA).

Evaluation of method error by calculating the reproducibility of the reference points

The method error associated with indicating the reference points on the 3D CT images (measured as an intra-observer and interobserver error) was evaluated for five randomly selected reference points by two authors (Kang and Park). Each author digitized the five reference points on 3D CT images, 20 times at 2-week intervals. The results were assessed using Dahlberg's formula as follows and analyzed statistically by intraclass correlation (ICC):

$$\text{Error}E_{(x \text{ or } y \text{ or } z)} = \sqrt{\sum[(x_n - x_{n-1})^2 \text{or} (y_n - y_{n-1})^2 \text{or} (z_n - z_{n-1})^2]/2N}$$

where x_n denotes the positional value of point x_n, and x_{n-1} does the positional value of point x_{n-1} in x coordinate.

Results

The results were first analyzed by two-way ANOVA, and all differences were found to be statistically insignificant ($p > 0.05$, detailed data not shown). The one-way ANOVA statistical analyses for each result are thus described later.

Reproducibility of the reference points

The intra-observer errors ranged between 0.2 and 0.9 mm for the x, y, and z coordinates. The ICC with 95% of confidence intervals for the (x, y, and z) coordinate system was found to be 0.993 ($p > 0.0001$) for the intra-observer reliability, and 0.939 ($p > 0.0001$) for the interobserver reliability.

***Table 1.* The definition of reference points that were used in this study**

Points	Full term (Definition)	Bilaterality
FM	Frontomaxillary Suture (Junction of frontomaxillary sutures at mid distance between anterior and posterior tops of maxillary processes)	√
M	M point (Junction of maxillary, nasal, and frontal sutures)	√
Clp	Clinoid process (Apex of the posterior clinoid process)	√
NP	Nasopalatine foramen (Anterior wall of nasopalatine foramen at the level of nasal floor)	
U1 tip	Tip of maxillary incisor (midpoint of #11 or 21 incisal edge)	
#16, #26 cusp	Cusp of maxillary first molar (Mesiobuccal cusp tip of #16 or #26 tooth)	√
FC	Foramen cecum (the most anterior and superior point of foramen cecum)	
CFM	Center of foramen magnum (midpoint of foramen magnum at the level of basion)	
OC	Optic canal (The most superior point of optic canal)	√
EC	Eye ball center (The center point of eye ball in sagittal, axial, and coronal plane)	√
FxCe	Falx cerebri (The point of falx cerebri near Bregma on the coronal section)	
Po	Porion (The most superior point of bony exterior auditory canal)	√
Or	Orbitale (The point on the inferior orbital wall at the level of EC)	√
ON	Optic nerve (The midpoint of optic nerve at the level of eyeball insertion)	√
S	Sella (The center point of sella turcica in sphenoid bone)	
L	Lens (Center point of lens on the three planes)	√
PMF	Pterygomaxillary fissure (The lower most point of pterygomaxillary fissure at the level of posterior nasal spine)	√
GWS	Greater wing of sphenoid (The point of intersection by the anterior-most extent of the greater wing of sphenoid and anterior cranial base)	√

***Table 2.* The constructed midsagittal, horizontal, coronal, and visual pathway-related reference planes used in this study**

Planes	Description
Midsagittal	The plane constructed by three points, including FC, CFM, and S (which was supplemented by FxCe or Bregma)
C3 (cranial plane 3)	The plane perpendicular to midsagittal plane and passing through two middle points of bilateral M and bilateral Clp
FH (Frankfort-horizontal)	The plane perpendicular to midsagittal plane and passing through two middle points of bilateral Or and Po
PM (posterior maxillary)	The plane perpendicular to midsagittal plane and passing through two middle points of bilateral PMF and GWS
Occlusal	The plane perpendicular to midsagittal plane and passing through U1 tip and the middle point of bilateral Mx 6 cusp tip
CF1 (craniofacial plane 1)	The plane perpendicular to midsagittal plane and passing through NP and middle point of bilateral FM
OAP (orbital axis plane)	The plane constructed by three points including the right and left EC and middle point of bilateral OC
VAP (visual axis plane)	The plane constructed by three points including the right and left EC and middle point of bilateral ON
OpAP (optical axis plane)	The plane constructed by three points including the right and left L and middle point of bilateral ON

Angles between MS and the vision-based planes or lines

The angles formed between the MS and vision-based planes were almost 90°, and they did not differ significantly between groups I, II, and III, or between the three vision-related planes (Table 3). In contrast, the angles between the MS and the OA in group I and VA in group III had normal values close to 22.5°; the others, and especially the OpA, exhibited larger or smaller values. A statistically significant intergroup difference was found only for OA, being highest in group III. All of the vision-based lines differed significantly between the groups at the 99% level of

Table 3. **Angles (in degrees) between the midsagittal (MS) and horizontal planes and lines**

	MS				MS			
Group	OAP	VAP	OpAP	*p*	OA	VA	OpA	*p*
I	90.1 ± 0.7	89.9 ± 0.7	89.0 ± 1.6	0.23	22.8 ± 1.8	23.1 ± 3.5	14.4 ± 2.2	<0.001
II	90.1 ± 0.4	89.9 ± 1.4	90.3 ± 1.3	0.64	24.1 ± 1.8	22.1 ± 3.2	15.0 ± 2.8	<0.001
III	90.1 ± 1.0	90.2 ± 1.3	90.4 ± 1.4	0.73	25.4 ± 0.4	22.4 ± 2.2	16.6 ± 1.6	<0.001
p	0.97	0.69	0.06		0.004	0.73	0.053	

Results of the one-way ANOVA and *post hoc* Scheffe's statistical tests.
OAP, orbital axis plane; VAP, visual axis plane; OpAP, optical axis plane; FH, Frankfort horizontal.

significance (one-way ANOVA); OA and VA were significantly larger than the OpA (*post hoc* Scheffe's analysis; Table 3).

Angles measured between the PM and vision-based planes

The angles between the PM and vision-based planes ranged between 86.4° and 92.9° (Table 4). The PM–OAP angle was almost 90° (range 89.5–90.9°) and differed significantly between groups III and II ($p = 0.011$, group III > group II; Scheffe's method). However, the angles between the PM and OpAP or VAP did not differ significantly between the three groups. The C3 and FH planes exhibited a smaller angulation (range 87.2–89.9°) with the PM plane than did the OAP. There were no statistically significant differences between the angles subtended by the PM plane and C3, FH, and OAP.

Angles between the vision-based planes and other reference planes including C3, CF1, FH, and the occlusal plane

The angles between the vision-based planes and other reference planes including C3, FH, CF1, and the occlusal plane were evaluated (Table 5). The angle between C3 and the OAP was 2.7 ± 1.8° (mean ± standard deviation), 3.9 ± 1.7°, and 4.3 ± 2.1° in groups I, II, and III, respectively; there were no statistically significant intergroup differences ($p = 0.157$). The angle between C3 and the VAP or OpAP was larger than that between C3 and the OAP, and it was statistically significant only for group II ($p = 0.01$, VAP and OpAP > OAP by Scheffe's *post hoc* analysis).

The angle between FH and the OAP ranged from 3.2° to 3.8° (without statistically significant intergroup differences). Furthermore, the angle subtended by FH and the VAP or OpAP differed significantly from that subtended by FH and the OAP for group II ($p = 0.003$, VAP and OpAP > OAP by Scheffe's method). The angle between CF1 and the OAP was 88.8, 88.1, and 85.7° in groups I, II, and III, respectively, with no statistically significant intergroup differences. And the angle between the OAP and the occlusal plane was 8.5 ± 4.6°, 12.5 ± 6.5°, and 5.8 ± 3.4° in groups I, II, and III, respectively ($p = 0.002$).

Table 4. **Angles (in degrees) between the posterior maxillary (PM) plane and the horizontal planes**

	PM				PM			
Group	OAP	VAP	OpAP	*p*	OAP	C3	FH	*p*
I	90.3 ± 0.6	92.9 ± 6.2	92.3 ± 5.4	0.517	90.3 ± 0.6	88.9 ± 4.0	89.9 ± 5.0	0.741
II	89.5 ± 1.3	91.1 ± 10.4	90.1 ± 10.4	0.876	89.5 ± 1.3	87.2 ± 4.1	88.2 ± 3.8	0.213
III	90.9 ± 1.3	86.4 ± 9.1	88.3 ± 8.1	0.157	90.9 ± 1.3	89.3 ± 4.2	89.8 ± 3.7	0.317
p	0.011	0.167	0.504		0.011	0.379	0.466	

Results of the one-way ANOVA and *post hoc* Scheffe's statistical tests.
OAP, orbital axis plane; VAP, visual axis plane; OpAP, optical axis plane; FH, Frankfort horizontal.

Table 5. **Angles (in degrees) between the visual pathway-related planes and the horizontal (C3 and FH) or other reference planes**

Group	C3				FH				CF1				Occlusal plane			
	OAP	VAP	OpAP	*p*	OAP	VAP	OpAP	*p*	OAP	VAP	OpAP	*p*	OAP	VAP	OpAP	*p*
I	2.7 ± 1.8	5.1 ± 3.3	5.1 ± 2.4	0.126	3.3 ± 2.4	6.1 ± 3.5	4.6 ± 2.7	0.188	88.8 ± 5.0	93.3 ± 8.1	91.4 ± 6.2	0.414	8.5 ± 4.6	11.3 ± 7.2	10.4 ± 6.3	0.654
II	3.9 ± 1.7	8.6 ± 4.1	8.3 ± 6.2	0.01	3.2 ± 2.4	8.0 ± 2.9	6.9 ± 5.0	0.003	88.1 ± 7.6	90.1 ± 12.4	90.7 ± 12.5	0.8	12.5 ± 6.5	14.3 ± 7.6	14.0 ± 6.7	0.761
III	4.3 ± 2.1	6.8 ± 6.9	8.0 ± 6.5	0.131	3.8 ± 2.2	6.6 ± 6.7	6.9 ± 5.6	0.146	85.7 ± 8.1	85.8 ± 9.2	87.8 ± 8.4	0.691	5.8 ± 3.4	8.6 ± 6.0	7.7 ± 4.6	0.191
p	0.157	0.341	0.437		0.735	0.607	0.512		0.518	0.194	0.586		0.002	0.07	0.012	

Results of the one-way ANOVA and *post hoc* Scheffe's statistical tests.
OAP, orbital axis plane; VAP, visual axis plane; OpAP, optical axis plane; FH, Frankfort horizontal.

Discussion

The NHP is defined as the normal balanced position of the head adjusted naturally when it is turning to an object in the distance at the horizon. The head position is adjusted by the reflex system of the head (30, 31) and affected by various physical stimuli (32–34). The importance of visual reflex or gaze for the NHP is evidenced in that the head position of a visual disability group is tilted lower by as much as 4.3° and the neck is inclined by 4.5° more to the anterior than that of normally sighted subjects (32). The upright stance and walking posture of humans is also important to bring the head into the NHP with the VA facing forward. In addition, the head position and VA induce a unique pattern of growth and development in the face and head (20). Thus, we could deduce that the gaze-related reference plane is advantageous for the expression of the NHP.

The morphology of the orbit, optic canal, and its surrounding structures at the anterior cranial base change very little during the active growth period (35, 36). Various reference planes of the orbit have been suggested, and the optic plane is such a plane that bisects the supraorbital and infraorbital rim (37). The NOP, which runs from the lens of the eyeball to optic canal, maintains the horizontal orientation (24, 38) and OA, passing through the orbit and the eyeballs, runs a relatively horizontal course in mammals (16).

In the present study, we evaluated three visual pathway-related lines (OA, VA, and OpA) and planes (OAP, VAP, and OpAP). The OA generally forms an angle of 22.5° with the MS plane or its parallel medial orbital wall (22). Our analysis revealed that the OA in group I and the VA in groups II and III had angles near to 22.5°. And the OAP appeared to form an angle of 90.1° with MS plane for all three groups without intergroup differences ($p = 0.97$). So it seems that the OA and OAP may be more appropriate than the other two planes.

Enlow and Moyers (25) stated that the PM plane is a natural anatomic and morphogenetic plane that can express the relationship between the cranium, the pharynx, and the face and forms a right angle with the neutral horizontal axis of the orbit, which corresponds to the OA in all kinds of mammals. And it can be constructed on 3D radiographs by drawing a line connecting the most posterior–inferior point of the maxillary tuberosity and the average point on the anterior-most extent of the GWS (20, 39). We adopted this for use in 3D images and validated that the OAP subtended an angle of almost 90° with the PM plane, with statistically significant intergroup differences, whereby the angles tended to be larger in group III than in group II. This may imply that the mandibular prognathic subjects have higher visual axes than the retrognathic subjects, or may have a more posteriorly angulated PM plane.

When we wanted to understand the other possible expressions of the NHP, the angle between the FH plane and the OAP was 3.2–3.8°, and that was similar between C3 and the OAP (2.7–4.3°). It has already been variously reported that the angle between the FH plane and true horizontal, OAP or NOP is $0.63 \pm 2.33°$ (3), $1.3 \pm 5°$ (40), 5° (on sitting) (41), or 7° (38). Although our results also varied from these previous findings, it seems clear that FH makes angles around 5° to the OAP-related orbital plane or true horizontal plane.

For Delaire's craniofacial analysis (1, 4, 29), C3 plane is a superior horizontal reference plane and CF1 describes the anterior craniofacial balance. CF1 is normally perpendicular to C3 with a registration at point FM (for adult men), and the angle between them generally expresses the anterior–posterior maxillary position. Although the intergroup difference was not statistically significant, the measured angle between the OAP and CF1 tends to be larger in groups I and II than in group III. And the order according to the magnitude of angles between the occlusal plane and OAP or OpAP was group II > group I > group III with the statistical significance. This finding concurs with the general understanding of maxillofacial dysmorphology and with those of previous studies (42, 43).

Conclusions

We constructed and validated the vision-related planes, the OAP, VAP, and OpAP, by evaluating the relationship between reference planes including CF1, the occlusal, PM, and MS plane on 3D CT images. The OAP, not the VAP and OpAP, maintained the ideal relationship with the MS and PM planes more accurately and properly described the different patterns of maxillofacial dysmorphology with CF1 and the occlusal plane. Our findings confirmed that the visual axis-related plane, especially OAP, fits the definition of the vision-based plane and can help to depict the orientation of the head, which is necessary during 3D analysis of maxillofacial dysmorphology or anthropology with CT images.

Clinical relevance

Rapid advances in 3D visualization technology have improved the analysis of craniofacial structures, which were hard to observe using 2D imaging techniques. We introduced and evaluated the visual pathway-based horizontal reference planes for 3D craniofacial analysis. From these results, we could understand that they were acceptably accurate, and especially, the orbital axis planes can be used for the 3D craniofacial analysis of patients with dysmorphology or for anthropological measurements.

Acknowledgements: This study was supported by a grant from the Korea Healthcare Technology R and D Project, Ministry for Health, Welfare, and Family Affairs (A101625) for LSH. We thank MK Kim for the critical readings of this manuscript and the helpful discussions.

Conflict of interests

We declare that we have no conflict of interest.

References

1. Delaire J, Schendel SA, Tulasne JF. An architectural and structural craniofacial analysis: a new lateral cephalometric analysis. *Oral Surg Oral Med Oral Pathol* 1981;52:226–38.
2. Burstone CJ, James RB, Legan H, Murphy GA, Norton LA. Cephalometrics for orthognathic surgery. *J Oral Surg* 1978;36:269–77.
3. Sassouni V. A roentgenographic cephalometric analysis of cephalo-facial-dental relationships. *Am J Orthod* 1955;41:735–64.
4. Olszewski R, Cosnard G, Macq B, Mahy P, Reychler H. 3D CT-based cephalometric analysis: 3D cephalometric theoretical concept and software. *Neuroradiology* 2006;48:853–62.
5. Olszewski R, Zech F, Cosnard G, Nicolas V, Macq B, Reychler H. Three-dimensional computed tomography cephalometric craniofacial analysis: experimental validation in vitro. *Int J Oral Maxillofac Surg* 2007;36:828–33.
6. Terajima M, Yanagita N, Ozeki K, Hoshino Y, Mori N, Goto TK et al. Three-dimensional analysis system for orthognathic surgery patients with jaw deformities. *Am J Orthod Dentofacial Orthop* 2008;134:100–11.
7. Olszewski R, Tanesy O, Cosnard G, Zech F, Reychler H. Reproducibility of osseous landmarks used for computed tomography based three-dimensional cephalometric analyses. *J Craniomaxillofac Surg* 2010;38:214–21.
8. Cavalcanti MG, Haller JW, Vannier MW. Three-dimensional computed tomography landmark measurement in craniofacial surgical planning: experimental validation in vitro. *J Oral Maxillofac Surg* 1999;57:690–4.
9. De Momi E, Chapuis J, Pappas I, Ferrigno G, Hallermann W, Schramm A et al. Automatic extraction of the mid-facial plane for cranio-maxillofacial surgery planning. *Int J Oral Maxillofac Surg* 2006;35:636–42.
10. Katsumata A, Fujishita M, Maeda M, Ariji Y, Ariji E, Langlais RP. 3D-CT evaluation of facial asymmetry. *Oral Surg Oral Med Oral Pathol Oral Radiol Endod* 2005;99:212–20.
11. Cooke MS, Wei SH. A summary five-factor cephalometric analysis based on natural head posture and the true horizontal. *Am J Orthod Dentofacial Orthop* 1988;93:213–23.
12. Cooke MS. Five-year reproducibility of natural head posture: a longitudinal study. *Am J Orthod Dentofacial Orthop* 1990;97:489–94.
13. Petricevic N, Celebic A, Celic R, Baucic-Bozic M. Natural head position and inclination of craniofacial planes. *Int J Prosthodont* 2006;19:279–80.
14. Matsumoto S. A new coordinate system using the orbital axis for morphological analysis of primate skulls. *Primates* 1983;24:546–56.
15. Moorrees C, Kean M. Natural head position, a basic consideration in the interpretation of cephalometric radiographs. *Am J Phys Anthropol* 1958;16:213–34.
16. Barbera AL, Sampson WJ, Townsend GC. An evaluation of head position and craniofacial reference line variation. *Homo* 2009;60:1–28.
17. Cole SC. Natural head position, posture, and prognathism: the Chapman Prize Essay, 1986. *Br J Orthod* 1988;15:227–39.
18. Moorrees CF. Natural head position – a revival. *Am J Orthod Dentofacial Orthop* 1994;105:512–3.
19. Madsen DP, Sampson WJ, Townsend GC. Craniofacial reference plane variation and natural head position. *Eur J Orthod* 2008;30:532–40.
20. Enlow D, Hans M. *The Plan of the Human Face. Essentials of Facial Growth*. Philadelphia: Saunders; 1996. pp. 146–54.
21. Douglas R, Lawrenson J, Ruskell G. *The Eye. Gray*'s Anatomy: The Anatomical Basis of Clinical Practice, 40th edn. London: Churchill Livingstone; 2008. P. 696.
22. O'Rahilly R. The Orbit. In: Gardner E, Gray D, O'Rahilly R, editors. *Anatomy: A Regional Study of Human Structure*, 4th edn. London: W.B. Saunders; 1975. pp. 628–30.
23. Tamraz J. Neuroradiologic investigation of the visual system using magnetic resonance imaging. *J Clin Neurophysiol* 1994;11:500–18.
24. Cabanis EA, Iba-Zizen MT, Coin JL, Guillaumat L, Pineau H. Visual pathways, a ''new'' plane of orientation of the head (neuro-ocular plane). *Bull Soc Ophtalmol Fr* 1981;81:433–9.
25. Enlow DH, Moyers RE. Growth and architecture of the face. *J Am Dent Assoc* 1971;82:763–74.
26. Rohrschneider K. Determination of the location of the fovea on the fundus. *Invest Ophthalmol Vis Sci* 2004;45:3257–8.
27. Williams TD, Wilkinson JM. Position of the fovea centralis with respect to the optic nerve head. *Optom Vis Sci* 1992;69:369–77.
28. Kim H. *Reference Plane for Craniofacial Analysis with Three-Dimensional Computed Tomography (3D CT)*. Seoul: Yonsei University; 2005.
29. Kil T, Choi J, Kim B, Park W, Yi C, Lee S. A proposal for 3D craniofacial analysis by Delaire's method. *J Korean Assoc Oral Maxillofac Surg* 2009;35:236–7.
30. Cuccia AM, Caradonna C. The natural head position. Different techniques of head positioning in the study of craniocervical posture. *Minerva Stomatol* 2009;58:601–12.
31. Cuccia AM, Carola C. The measurement of craniocervical posture: a simple method to evaluate head position. *Int J Pediatr Otorhinolaryngol* 2009;73:1732–6.
32. Fjellvang H, Solow B. Craniocervical postural relations and craniofacial morphology in 30 blind subjects. *Am J Orthod Dentofacial Orthop* 1986;90:327–34.
33. Solow B, Sonnesen L. Head posture and malocclusions. *Eur J Orthod* 1998;20:685–93.
34. Luyk NH, Whitfield PH, Ward-Booth RP, Williams ED. The reproducibility of the natural head position in lateral cephalometric radiographs. *Br J Oral Maxillofac Surg* 1986;24:357–66.
35. Belden CJ, Mancuso AA, Kotzur IM. The developing anterior skull base: CT appearance from birth to 2 years of age. *AJNR Am J Neuroradiol* 1997;18:811–8.
36. Standerwick RG, Roberts WE. The aponeurotic tension model of craniofacial growth in man. *Open Dent J* 2009;3:100–13.
37. Tremont TJ. An investigation of the variability between the optic plane and Frankfort horizontal. *Am J Orthod* 1980;78:192–200.
38. Tamraz J, Comair Y. *Cephalic Reference Lines Suitable for Neuroimaging. Atlas of Regional Anatomy of the Brain using MRI with Functional Correlations*. Berlin: Springer; 2006. pp. 268–71.
39. McCarthy RC, Lieberman DE. Posterior maxillary (PM) plane and anterior cranial architecture in primates. *Anat Rec* 2001;264:247–60.

40. Downs W. Analysis of the dentofacial profile. *Angle Orthod* 1956;26:191–212.
41. Ferrario VF, Sforza C, Miani A, Tartaglia G. Craniofacial morphometry by photographic evaluations. *Am J Orthod Dentofacial Orthop* 1993;103: 327–37.
42. Kim IH, Yi CK. Architectural and structural craniofacial analysis of Korean adults. *J Korean Assoc Oral Maxillofac Surg* 1991;17:33–44.
43. Hong SX, Yi CK. A classification and characterization of skeletal Class III malocclusion on etio-pathogenic basis. *Int J Oral Maxillofac Surg* 2001;30:264–71.